



# Effect of tool geometry on friction stir butt-welding of AA6061-T6 alloy: Part 1 - Numerical Study

تأثير الشكل الهندسي للأداة المستخدمة لإنتاج وصلة لحام تناكبية بطريقة الدمج الإحتكاكي لسبيكة AA6061-T6 : الجزء الأول - دراسة عددية

Abdallah A. Elsherbiny, Tawakol A. Enab, Ahmed M. Galal and Magdy S. Ghattas

## KEYWORDS:

Friction Stir Welding (FSW); Butt welding; Aluminum alloy; Finite Element Method (FEM); Coupled Eulerian Lagrangian (CEL) approach.

**المخلص العربي:-** هذا البحث يقدم محاكاة لعملية لحام الدمج الإحتكاكي لسبيكة ألومنيوم (AA6061-T6). عملية المحاكاه هذه تتم بالدمج بين طريقة لاجرانج وطريقة أويلر باستخدام برنامج أباكوس وذلك للتغلب على المشاكل التي تحدث في الشبكة المستخدمه أثناء التحليل. تتم عملية لحام الدمج الإحتكاكي في ثلاث مراحل فالمرحلة الأولى هي عملية الغرز تليها المرحلة الثانية وهي الدوران لمدته زمنية محددة حتى الوصول للتعجن الكامل للمعدن يليها المرحلة الأخيرة وهي الحركة الطولية لأداة اللحام لإنتاج خط اللحام. بعد بناء النموذج الكامل لعملية المحاكاة تمت دراسة تأثير الشكل الهندسي لأداة اللحام المستخدمة وتأثيرها على التوزيع الحراري والإجهادات المتولدة في المعدن.

**Abstract—** The current paper presents a numerical study on friction stir butt-welding of Aluminum alloy (AA6061-T6). The effect of pin geometry on the developed temperature and distributions of stresses at welding zone has been investigated. Seven tool geometries were simulated with coupled thermo-mechanical three-dimensional finite element models developed

using Coupled Eulerian Lagrangian (CEL) method at ABAQUS® software V.6.14. The welding process was simulated in three stages, i.e. plunge, dwell and finally welding step in which the tool was traveled with constant linear speed. The results show that the tool geometry has a significant effect on the distribution of temperatures and stresses developed at the welded zone. Moreover, comparing the results of the developed models and those of the previous studies a good coherence was achieved.

Received: 17 July, 2019 - Accepted: 9 September, 2019

Abdallah A. Elsherbiny, demonstrator at Production Engineering and Mechanical Design Department, Faculty of Engineering, Mansoura University, Mansoura, Egypt (Email: Abdallah.a.m@mans.edu.eg).

**Corresponding Author:** Tawakol A. ENAB, Associate Professor at Production Engineering and Mechanical Design Department, Faculty of Engineering, Mansoura University, Mansoura (Email: tenab@mans.edu.eg).

Ahmed M. Galal, Associate Professor at Production Engineering and Mechanical Design Department, Faculty of Engineering, Mansoura University, Mansoura, Egypt.

Magdy S. Ghattas, Emeritus Professor at Production Engineering and Mechanical Design Department, Faculty of Engineering, Mansoura University, Mansoura, Egypt.

## I. INTRODUCTION

**A**LUMINUM alloys have numerous applications. According to their pretty properties they used in space area and ships building. Weldability of aluminum alloys by conventional methods have many challenges as thermal conductivity of the aluminum alloys, using shielding gas, the current used (AC or DC), the design of joint, the position of welding, surface condition, and other challenges For example, when the conventional methods are used for aluminum welding the current type and the shielding

gas must be selected precisely to get maximum heat input to the joint to compensate the rapid heat dissipation [1]. The high dissipation resulted from high thermal conductivity of such alloys. In addition, the produced residual stresses by conventional methods are greater.

To overcome those challenges a new technique of solid joining process was feigned in 1991 at The Welding Institute (TWI) in England which is friction stir welding (FSW) [1-3]. This technique mostly used with aluminum alloys because of attractive mechanical properties like dynamic and fatigue strength, low defects in the welding joint. In addition to welding dissimilar materials there are many significant advantages of FSW in engineering applications which are using only about 2.5% of energy of laser and electron beam welding do not need filler metal, do not need heat treatment, also do not need shielding gas, good dimensional stability [1].

The investigation of friction stir process parameters is crucial to get a welded joint with high quality. The main concept of friction stir welding process is using a rotating inconsumable tool which rotates with constant speed and plunge into the material with fixed feed. This tool consists of two main parts, the first is the pin and the second is the shoulder. Each of these parts has a wide research field. The heat generated from the friction between the tool and the workpiece dissipated into work piece, tool and air [4]. The geometry of the welded joint depends on physical properties of the material that dependent on temperature, the heat sources distribution and geometry of pin and shoulder [5]. The experimental work is time consuming and costly so a numerical simulation was introduced to decrease the cost study if this process. To build a fully coupled thermo-mechanical model more than one approach can be used such as Arbitrary Lagrangian Eulerian (ALE), Coupled Eulerian Lagrangian (CEL) [6] and Spherical Particle hydrostatic (SPH) approach [7]. These techniques are used to avoid excessive deformation of the mesh or instability of the system. In this study, (CEL) technique was used to develop the model.

Seven tool geometry was investigated to get the optimal shape for the pin geometry in welding process.

## II. FRICTION STIR WELDING PROCESS

### a. Main steps of the process

FSW process can be performed in three main steps, plunge step, dwell or rotation step and feed step. The plunge step is the first step in which a rigid rotating tool plunges into a clamped work piece until the shoulder contact the upper surface of the workpiece. The pin extruded from tool shoulder rotates and results in the heat needed for softening material and performing weld. Finally, the generation of weld line produced from the tool feed. Most of heat is generated from friction between tool and specimen and others came from plastic deformation [1, 8]. Figure (1) is a schematic illustration of the three main steps of FSW.

### b. Welding process parameters

The parameters of welding and the tool geometry which is considered one of the most critical condition in FSW process govern the material flow and heat localizing. In addition the design of the welding joint has a significant effect on the material flow pattern and temperature distribution.

The tool which consists of pin and shoulder may have different geometries. In this search seven different pin geometries will be discussed (see figure (2)).

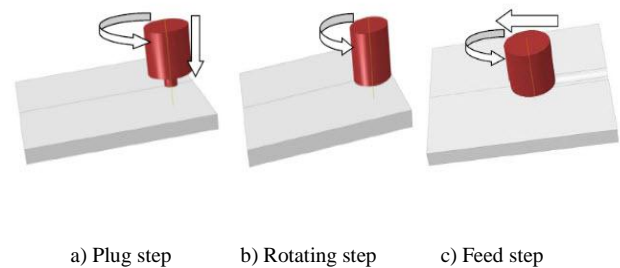


Fig. 1. The friction stir welding steps.

## III. NUMERICAL SIMULATION OF FSW

Simulation was carried out using Coupled Eulerian Lagrangian (CEL) method formulation encompassed in the FE code, ABAQUS Explicit V6.14. CEL approach was used to avoid excessive deformation of the mesh [2, 3, 8]. Simulations embody the three phases of the FSW process.

The tool is modeled as a linear-elastic Lagrangian body [2, 3, 8-10]. Each tool has a total pin length of 6 mm with shoulder of 20 mm diameter and pin of 6 mm major diameter. It rotates with an angular speed of 3000 rpm. The tool is represented in the model using C3D8RT element type [2, 3, 8, 11]. The two plates are modeled as Eulerian parts and meshed with EC3D8RT element type to enables the material flow. A gap between the sheets may be existed for a more realistic setup [2]. Figure (4) shows the mesh for both tool and workpiece.

The lower surfaces of the plates are completely fixed in the z-direction. Also, all planes normal to the x-direction are fixed. First, the tool plunges into the two sheets ( $V_z = 5$  mm/min) and rotates with a specified speed of 3000 rpm. After the dwelling phase, the tool was hold on for a second (i.e. dwelling time). Finally the planes normal to the y-direction are charged with a velocity ( $V_y = 5$  mm/min) to represent the linear speed as shown in figure (3). It is assumed that 100% of the friction converted into heat from which 85% flows into the aluminum plates [1-3, 12]. The ambient temperature is set to 20 °C. A dense mesh is very significant for detecting burrs or voids formation and material loss over the Eulerian domain but in the other hand the time will increase highly. Using moderate course mesh the time was very high so by performing study mesh the difference in results detected in definite range

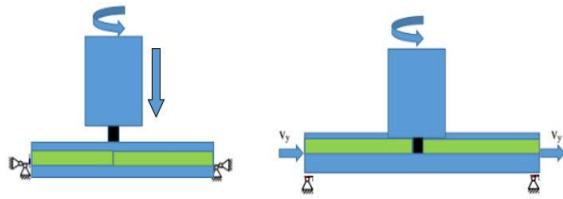
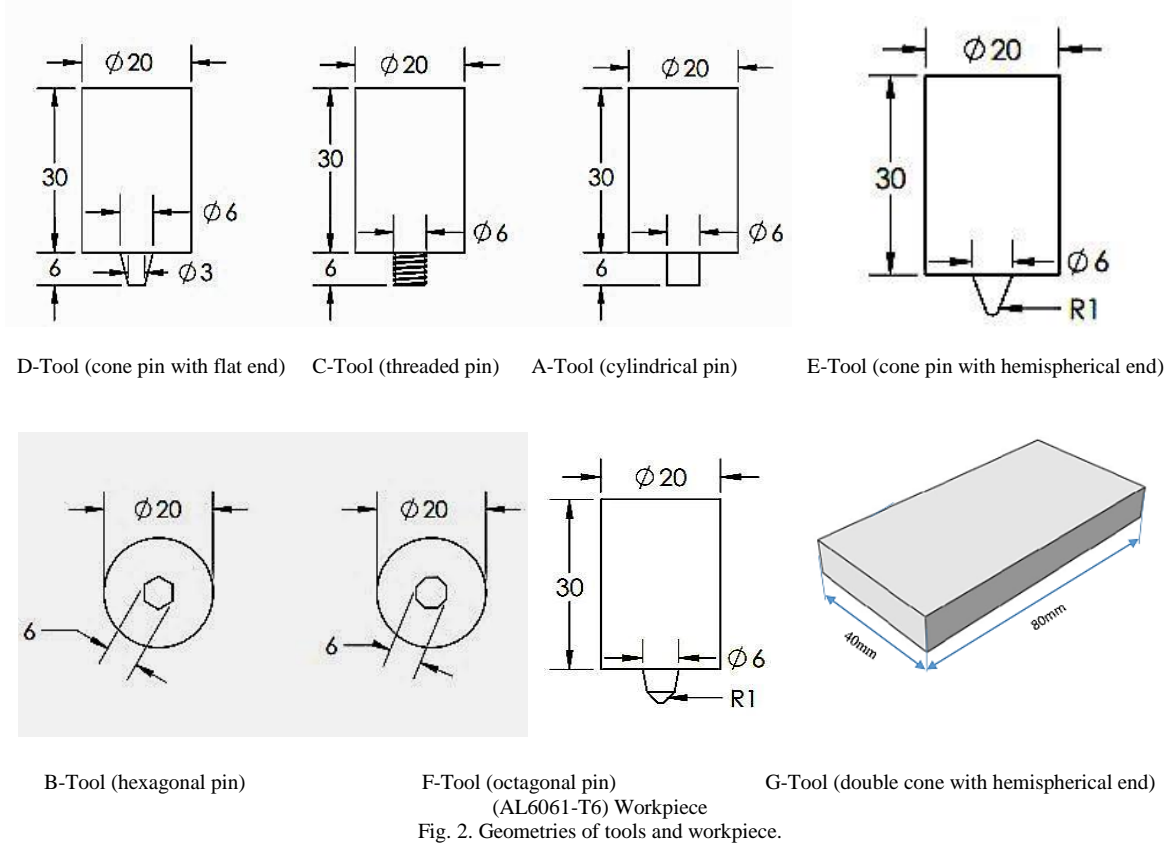


Fig. 3. Schematic model assembly.

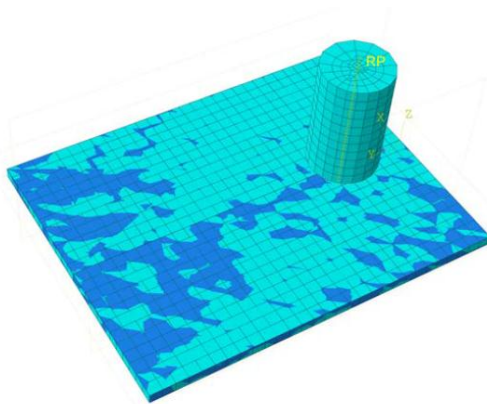


Fig. 4. (CEL) mesh for the rigid tool and the specimen

*a. Material properties*

Workpiece material modeled as elastic plastic Johnson-Cook for material modelling; as shown by equation (1); and the material assumed to be isotropic. Table (1) presents the Johnson-Cook constants for AA 6061-T6 [2, 3, 8, 9, 13]. While, tables (2) and (3) illustrate the mechanical and thermal properties of AA 6061-T6 and the thermal boundary conditions of the model respectively [2, 3, 8, 14].

$$\sigma_y = \left[ A + \frac{B}{(\epsilon^{pl})^{-n}} \right] \left[ 1 + C \ln \frac{\epsilon^{pl}}{\epsilon_o} \right] \left[ 1 - \left( \frac{T - T_{ref}}{T_{melt} - T_{ref}} \right)^m \right] \quad (1)$$

*b. Contact*

The contact between the tool and specimen is represented by Coulomb’s law of friction with coefficient of friction ( $\mu$ ) of 0.3 [2, 8]. The contact of model was defined with “ALL\* with self” which are automatic contact detection for every single node [2]. Both of normal and tangential forces are generated. There is a perfect (100%) sticking condition at the interface between the pin and the work piece.

TABLE I  
JOHNSON-COOK CONSTANTS FOR AA 6061-T6 [2, 3, 8, 14].

T <sub>melt</sub>	[°C]	583
A	[MPa]	293
B	[MPa]	121
C	Dimensionless	0.002
N	Dimensionless	0.23
M	Dimensionless	1.34

TABLE II  
TEMPERATURE DEPENDENT MATERIAL PROPERTIES FOR AA 6061-T6 [2, 3, 8, 14].

TEMPERATURE	C °	37.8	93.3	150	204	260	315
HEAT CONDUCTIVITY	W/M.C	162	177	184	192	201	207
SPECIFIC HEAT	J/KG.C	945	978	1004	1023	1052	1078
DENSITY	G/CM <sup>3</sup>	2.685	2.685	2.667	2.657	2.657	2.630
YOUNG'S MODULUS	GPA	68.54	66.19	63.09	59.16	53.99	47.48
YIELD STRENGTH	MPA	274.4	264.6	248.2	218.6	159.7	66.2
Thermal EXPANSION	*10-6 /C	23.45	24.61	25.67	26.6	27.56	28.53

TABLE III  
THERMAL BOUNDARY CONDITIONS OF THE MODEL [2, 3, 8, 14]

Thermal exchange between	Tool	Backing Plate	Tool shank	Ambient air (20°C)
workpiece	50000 W/m <sup>2</sup> .C	2000 W/m <sup>2</sup> .C	-	30 W/m <sup>2</sup> .C
Tool	-	-	2000 W/m <sup>2</sup> .C	20 W/m <sup>2</sup> .C
Backing plate	-	-	-	30 W/m <sup>2</sup> .C

IV. RESULTS AND DISCUSSION

The developed models predict the temperatures and stresses profiles along the welding path from starting until the steady state is reached. The temperature at the dwelling stage end is almost constant at the whole process. The formation of burrs behind the tool are similar to that formed in the front of the tool because of absence of the tilt angle. Also for the same reason the heat generation and temperature are equals at the front and heel side of the rigid tool.

The temperature and the stress fields are nearly symmetrical at the whole process. The assumption of heat transfer could be assumed as quasi-static steady condition. There are very important three regions in the field temperature, nugget zone (NZ), thermo-mechanically affected zone (TMAZ) and the heat affected zone (HAZ) as shown in

figure (5).

Nugget zone

Plastic distortion and frictional heating in FSW results in recrystallization the region surrounding the profile of the pin or the stirred zone. The grain sizes of this region are very fine and the shape of this region is controlled by the geometry of the pin, temperature of the workpiece, thermal conductivity of the parent material, vertical pressure, and composition of work piece [1].

Thermo-mechanically affected zone

It is the transient region between the nugget weld zone and the parent material. This region is characterized by structure which deformed excessively but there is no recrystallization occur because of insufficient deformation strain.

Heat affected zone

This region is beyond the thermo-mechanically affected zone and there is no plastic deformation but a thermal cycle. The HAZ has the same grain size of the parent material.

Figure (6) shows the temperature and stresses distributions for the different tool geometries. The optimal tool geometry is selected due to the maximum temperature, big area of nugget zone, minimum thermo-mechanical affected zone and heat affected zone. As shown in figure (5) the biggest nugget zone and maximum temperature come from tool with octagonal pin (tool F). Figure (7) shows the deformation in the material at the plunging and dwell steps. Moreover, it illustrates the deformation of burrs, so we built the Euler domain larger than the dummy part nearly by 4 mm. Figure (8) presents a comparison of the stresses and temperature profiles for the different modeled tool geometries. The profile of stresses and temperature are represented versus lateral distance to welding direction and this help us to determine the maximum nugget zone which lead to optimal selection of the tool geometry.

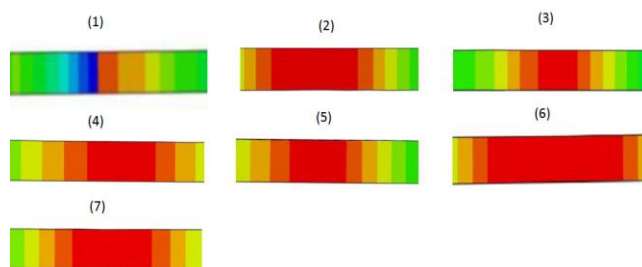


Fig. 5. The heat-affected zones for each too

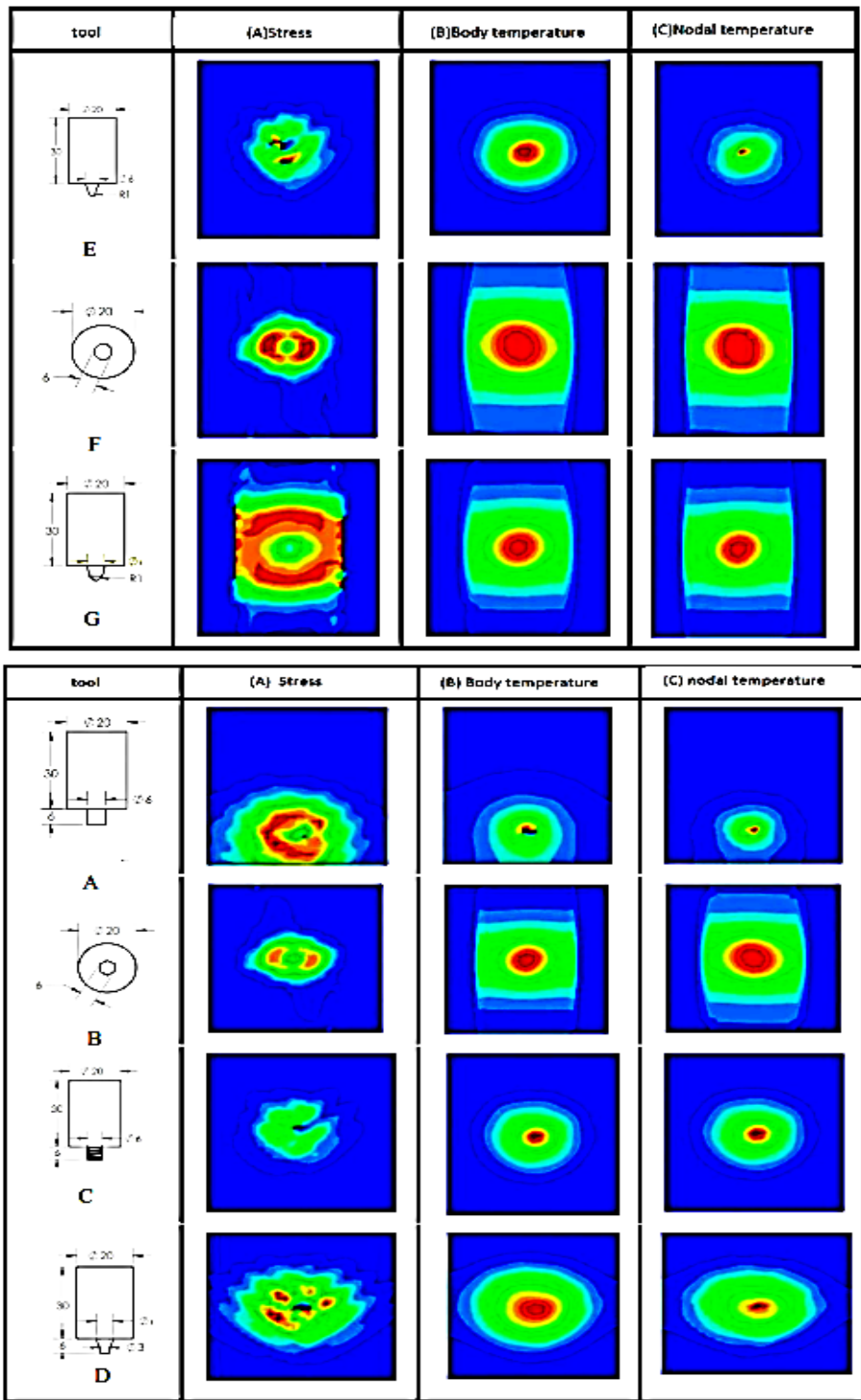


Fig. 7 Stress distribution, (B) Body temperature distribution and (C) Nodal temperature distribution

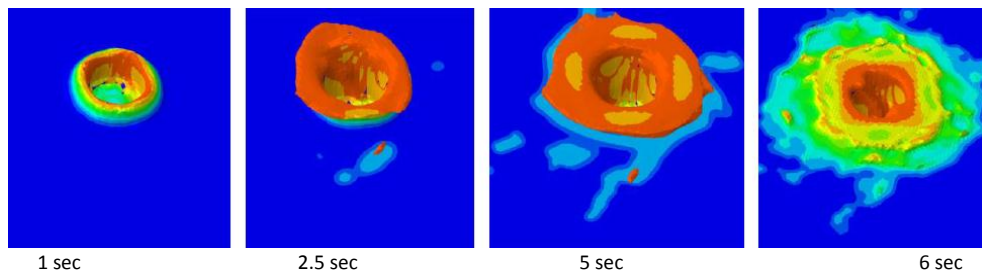


Fig. 7. The deformation with time in the plunge and dwell stages for tool (c)



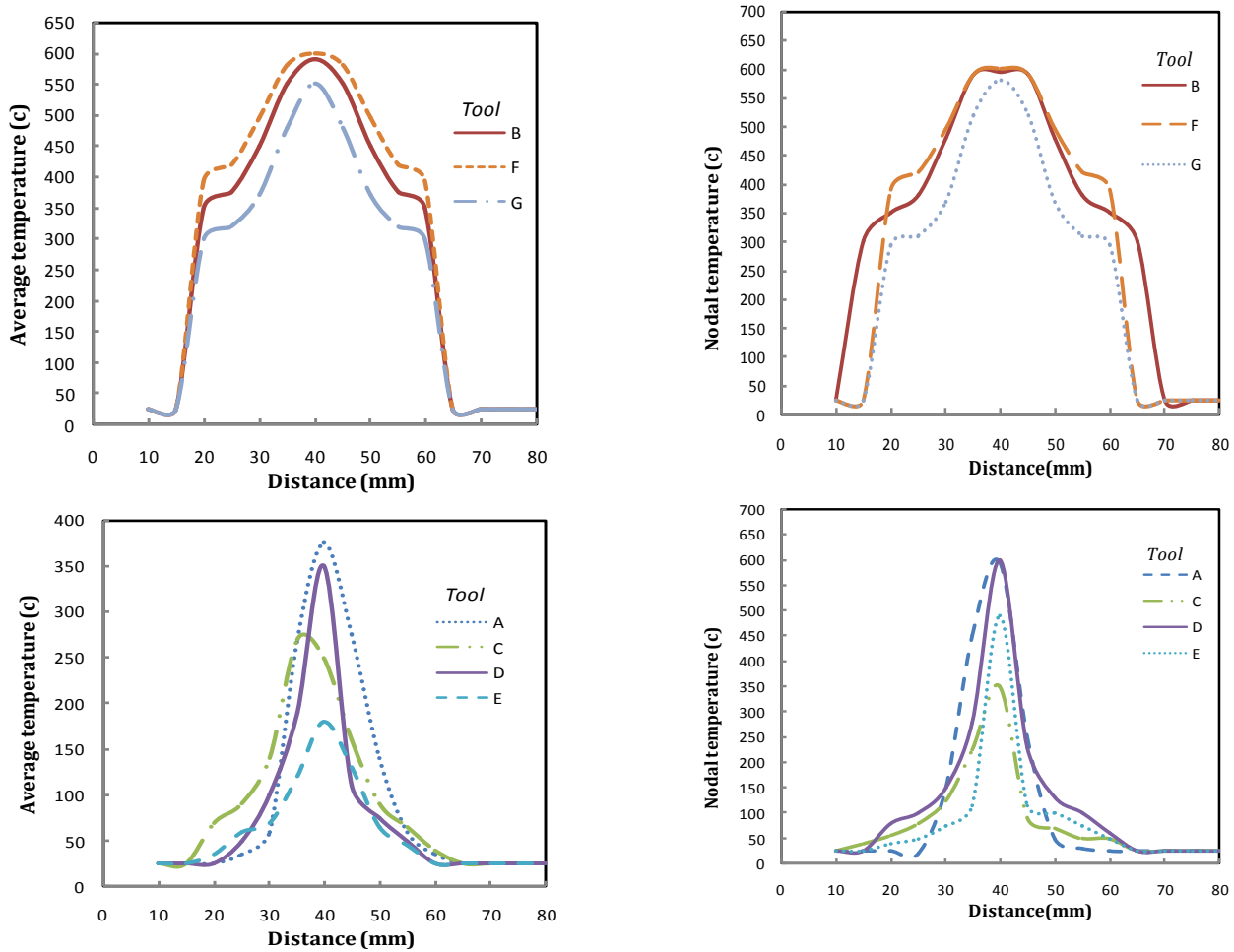


Fig. 8. The profiles of stresses and temperature

**V.CONCLUSIONS**

- The approach Coupled Eulerian Lagrangian (CEL) was used for modeling the FSW process in which complete coupled thermo-mechanical 3D FE model, for the whole
- Stages of the welding process was built up in ABAQUS Explicit V6.14.
- The results of the model were compared with other papers and the results achieved high agreement.
- The tool geometry has very important effect on the mechanical properties of stirred region, and the heat affected zone (HAZ) because each geometry gives a certain temperature and the mechanical properties are dependent temperature.
- Based on the maximum temperature and stress profiles the optimal pin geometry was the octagonal pin.

**REFERENCES**

[1] Mishra, R.S. and Z. Ma, Friction stir welding and processing. Materials Science and Engineering: R: Reports, 2005. 50(1): p. 1-78.  
 [2] Hossfeld, M. and E. Roos, A new approach to modelling friction stir welding using the CEL method. 2013.  
 [3] Hossfeld, M., A fully coupled thermomechanical 3D model for all phases of friction stir welding. 2016.

[4] Abhilash, J. and B.A. Apeksha, Simulation of friction stir welding using thermo-mechanical coupled finite element method. IOP Conference Series: Materials Science and Engineering, 2018. 455: p. 012113.  
 [5] Mijajlovic, M., D. Milcic, and M. Milcic, Numerical simulation of friction stir welding. Thermal Science, 2014. 18(3): p. 967-978.  
 [6] Meyghani, B., et al., Developing a Finite Element Model for Thermal Analysis of Friction Stir Welding by Calculating Temperature Dependent Friction Coefficient. 2017: p. 107-126.  
 [7] KirkFraser, L.K., LyneSt-Georges, Optimization of Friction Stir Weld Joint Quality Using a Mesh free fully-Coupled Thermo-Mechanics Approach. Molecular Diversity Preservation International 2018.  
 [8] Meyghani, B., et al. Developing a Finite Element Model for Thermal Analysis of Friction Stir Welding by Calculating Temperature Dependent Friction Coefficient. in 2nd International Conference on Mechanical, Manufacturing and Process Plant Engineering. 2017. Springer.  
 [9] Hamilton, R., D. MacKenzie, and H. Li, Multi-physics simulation of friction stir welding process. Engineering Computations, 2010. 27(8): p. 967-985.  
 [10] Kiral, B.G., M. Tabanoğlu, and H.T. Serindağ, Finite element modeling of friction stir welding in aluminum alloys joint. Mathematical and Computational applications, 2013. 18(2): p. 122-131.  
 [11] Guerdoux, S., Numerical simulation of the friction stir welding process. 2007, École Nationale Supérieure des Mines de Paris.  
 [12] Mishra RS, M.Z., Friction stir welding and processing. Mater Sci Eng R: Rep 2005: p. 50:1..78.  
 [13] Lammlein, D.H., Friction stir welding of spheres, cylinders, and t-joints: design, experiment, modelling, and analysis. 2010: Vanderbilt University.  
 [14] MatWeb, L., Matweb: material property data. línea]. Available: <http://www.matweb.com/search/DataSheet.aspx>, 2013.